"Bottleneck Effect" in Two-Dimensional Microfluidics

Patricia Burriel, Josep Claret, Jordi Ignés-Mullol, and Francesc Sagués

SOC and SAM Group, Departament de Química Física and Institut de Nanociència i Nanotecnologia de la UB (IN^2 UB), Universitat de Barcelona, Martí i Franquès 1, 08028 Barcelona, Spain

(Received 26 October 2007; published 2 April 2008)

An anomalously long transient is needed to achieve a steady pressurization of a fluid when forced to flow through micronarrowed channels under constant mechanical driving. This phenomenon, known as the "bottleneck effect" is here revisited from a different perspective, by using confined displacements of interfacial fluids. Compared to standard microfluidics, such effect admits in this case a neat quantitative characterization, which reveals intrinsic material characteristics of flowing monolayers and permits to envisage strategies for their controlled micromanipulation.

DOI: 10.1103/PhysRevLett.100.134503 PACS numbers: 47.61.−k, 68.18.−g

Microfluidics is a relatively new but already very promising field of study. Recent developments allow, for instance, to have unmatched control over size, shape, and composition of fluid droplets separated at the micron scale in multiphase flows [1]. Besides its impact in applied research, microscale flow phenomena reveal essential fluid features, somehow hidden under more conventional conditions. One remarkable observation, directly rooted in the compressible nature of the flowing material, has come to be known as the "bottleneck effect" [2,3]. It essentially consists in an anomalously long transient prior to steady pressurization of a fluid when made to flow through a microchannel under constant mechanical driving. Explicit references to this phenomenon are scarce (see [4], citing a private communication from Ulmanella *et al.*, and Martin *et al.* [5] for a reference in a chromatography context). In part this might be due to the presence of a similar but dominant transient arising purely from the elasticity of the confining tubes [2,3]. Here we propose a straightforward way to address separately the compressibility-originated bottleneck effect by reporting on "two-dimensional microfluidic" experiments employing confined flows in Langmuir monolayers, i.e., monomolecular insoluble films spread at the air-water interface [6]. The amphiphilic molecules easily modify their arrangement in the third dimension in response to changes in the lateral compression. This makes these systems intrinsically more compressible than their three-dimensional counterparts.

The study of flow properties of Langmuir monolayers, which are rheologically complex [7], is an issue of physical interest with large impact in biological and materials sciences [8]. Studies of interfacial shear and dilational rheology have been numerous in the past [9], but still deserve permanent attention [10]. In this context, a monolayer being forced to flow through a microchannel is a simple situation that has been quite often studied, both theoretically and experimentally, either to obtain viscoelastic parameters [11], to extract unusual velocity profiles [12–15], or to probe other non-Newtonian features in contraction-expansion flows [16]. Rather than looking at steady-state flow properties, as was done in the past, we will focus here on transient phenomena.

As a genuine signature of a bottleneck effect, we reproduce in Fig. 1(a) the temporal behavior of a Langmuir monolayer pushed to flow through a microchannel by a

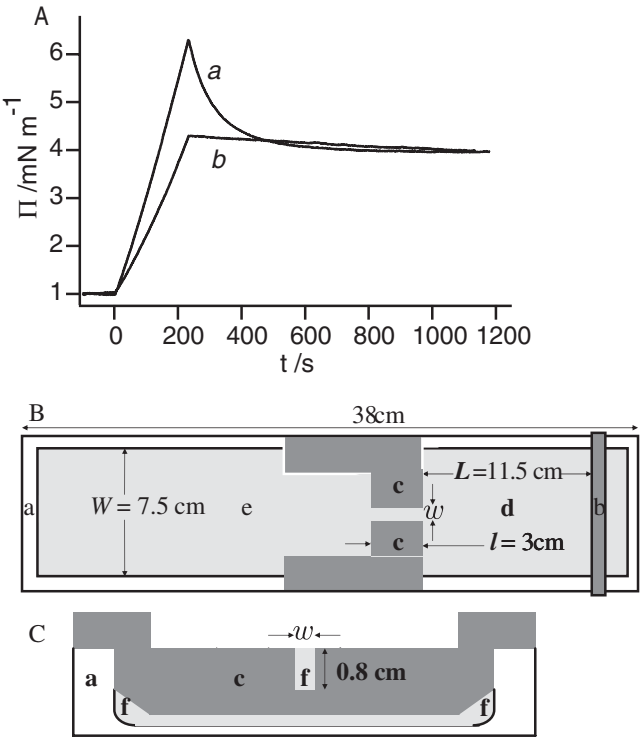

FIG. 1. (a) Evolution of the surface pressure in the compression chamber during a pressurization experiment of an elaidic acid Langmuir monolayer. (*a*) Flow through a channel 0.4 mm wide and 30 mm long. (*b*) Flow without channel. At $t = 200$ s, the moving barrier, $v_b = 10$ mm min^{-1}, is suddenly stopped. (b) Top view schematic diagram of the Langmuir trough and (c) perpendicular section of the channel assembly: (a) Teflon trough, (b) movable Delrin barrier, (c) black Delrin channel assembly, (d) compression chamber, (e) expansion chamber, (f) water subphase.

movable barrier (trace *a*). The monolayer is initially spread all over a custom-made Teflon cuvette separated in two compartments by a channel assembly made of black Delrin [Figs. 1(b) and 1(c)]. For the sake of comparison and with identical compression rate we monitor the evolution of a monolayer pressurized after removing the microchannel, i.e., in a cuvette of constant section (trace *b*). Elaidic acid (*trans*-9-octadecenoic) (Fluka, >99%) was chosen as a surfactant because of the wide range of temperature and surface pressures where it presents a featureless liquid expanded phase [17–19]. Water (18.2 MΩ cm) is supplied by a Millipore MilliQ system. Temperature is fixed at 20 °C. In the first case (trace *a*), the registered surface pressure Π steeply increases as long as the barrier is moving. Later on when the driving is suddenly stopped, Π decreases slowly until reaching a steady value. When the monolayer is pumped without contraction with the same compression rate and for the same time, Π increases more slowly (trace *b*). When the final reference condition is attained and the barrier is stopped, Π remains fixed thereafter [20]. The distinctive long transient in trace *a*, similarly to its three-dimensional counterpart, is thought to be generic, and we have observed that it depends only on the material parameters and geometrical factors of the constrained flow (see below). Essentially it can be thought of as a slow response of the squeezed material to a sudden change of its driving regime. We thus choose to address the contrary protocol, i.e., when the monolayer is suddenly set to motion from rest, a situation that admits a simpler theoretical description and a better analysis of experimental data.

Along with a study of transients in Π inside the compression chamber, we monitor the monolayer velocity inside the microchannel v_c by means of particle tracking with a CCD camera after seeding the monolayer with sulfur powder [16,21] and illuminating with an halogen light source. Flow images are analyzed using the public domain software ImageJ [22].

Under certain flow regimes, one can relate v_c to the pressure difference along the microchannel in terms of a permeability constant λ whose value is strongly dependent on the coupling between monolayer and subphase flows [13]. We will thus begin with an analysis of the flow profile inside the microchannel with the goal of correlating transients in Π and in v_c. Our measurements with a microchannel of length l and width w are consistent with a semielliptical velocity profile (Fig. 2), suggesting that monolayer flow is limited by the viscosity of the subphase μ_s [13]. In this case, one can express λ (measured by comparing the maximum velocity across the channel to pressure differences along it) as [13]

$$\lambda = \frac{w}{2\mu_s l}. \tag{1}$$

Since all parameters are known, we can validate this relationship for our data (inset of Fig. 2), showing that we do have a well-defined velocity regime in the monolayer flow.

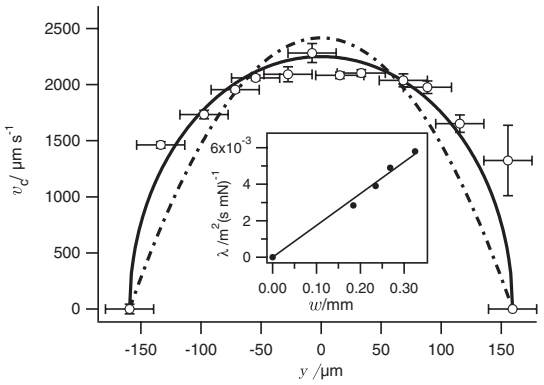

FIG. 2. Velocity profile across a channel of width 0.35 mm, and $v_b = 1.0$ mm min^{-1}. The coordinate y is the position from the center of the channel. A semielliptical (solid line) and a parabolic (broken line) profile are fitted to the data [13]. Inset: Dependence of the permeability λ vs w.

We will proceed with a brief theoretical analysis of the bottleneck effect in this system [3]. Let us thus consider a constant section cuvette divided into two compartments at a steady and uniform surface pressure Π_0. One of the compartments is designed as a compression chamber of (length) × (width) ($L \times W$), limited on one side by a barrier and contracted at the other end by a narrow microchannel. The second compartment is the expansion chamber of the monolayer after being squeezed [Figs. 1(b) and 1(c)]. At $t = 0$, the barrier is abruptly set to motion with fixed velocity v_b. We assume a planar, essentially unidirectional flow of the monolayer at the compression chamber, described by [23]

$$\mu \frac{\partial^2 v(x;t)}{\partial x^2} - \frac{\partial \Pi(x;t)}{\partial x} + \mu_s \frac{\partial v_s(x,z;t)}{\partial z}\bigg|_{z=0} = 0, \tag{2}$$

where subindex s refers to the shear viscosity and flow velocity of the subphase (strongly coupled to the monolayer flow, as shown above). The quantities without subindex apply to the monolayer, $z = 0$ corresponds to the monolayer level of the subphase flow, and x denotes the longitudinal (streamwise) direction with $x = 0$ the initial barrier position. In this geometry, the monolayer viscosity is a combination of the shear and the dilational viscosities, the latter being orders of magnitude larger than the former at small strain rates, $\mu = \mu_{\mathrm{sh}} + \mu_d \simeq \mu_d$.

Equation (2) is coupled to the continuity condition,

$$\frac{\partial \rho(x;t)}{\partial t} + \frac{\partial(\rho v)}{\partial x} = 0. \tag{3}$$

Surface pressure and density ρ are simply related in terms of the compressibility of the monolayer κ,

$$\frac{\partial \Pi}{\partial \rho} = \frac{1}{\kappa \rho}. \tag{4}$$

Integrating Eq. (2) and using Eqs. (3) and (4), we arrive at

$$\Pi + \mu\kappa\left(\frac{\partial \Pi}{\partial t} + v\frac{\partial \Pi}{\partial x}\right) - \mu_s \int^x \frac{\partial v_s}{\partial z}\bigg|_{z=0} dx = f(t). \tag{5}$$

The second term on the left-hand side is, at least, two orders of magnitude smaller than Π [24], and can be neglected. The third term is of the order of 10^{-3} mN m^{-1} for centimeter-long barrier displacements, and it can be also neglected. In conclusion, Π, and thus ρ, can be considered uniform but time-dependent during compression. Equations (2) and (3) can be combined to relate the temporal variation of Π to the spatial gradients of v, which we compute in terms of v_b and the value of v at the entrance of the channel. Flow conservation allows one to relate v to the velocity inside the channel v_c. We integrate the resulting differential equation, restricting to the early stages of compression when the surface pressure in the expansion area can be considered equal to the initial value Π_0 (Fig. 3), and writing v_c in terms of λ [i.e., $v_c(t) = \lambda(\Pi(t) - \Pi_0)$], to obtain

$$\Pi(t) = \Pi_0 + \frac{W}{w}\frac{v_b}{\lambda}[1 - \exp(-t/\tau)] \tag{6}$$

$$v_c(t) = \frac{W}{w} v_b [1 - \exp(-t/\tau)] \tag{7}$$

in terms of a time constant τ,

$$\tau = \frac{W}{w}\frac{\kappa L}{\lambda} = 2\mu_s \kappa \frac{WLl}{w^2}. \tag{8}$$

We can thus evaluate τ from geometrical and material parameters. In the range of surface pressures of our experiments, Π versus molecular area isotherms yield a typical value for the compressibility $\kappa = 5.3 \times 10^{-2}$ m mN^{-1}. For experiments with $w = 0.4$ mm (325 μm effective width, after taking into account the narrowing due to sticking of sulfur particles on the walls of the microchannel), we find $\tau = 270 \pm 30$ s. This value is in good agreement with the transient time of the relaxation-to-rest experiment shown in Fig. 1(a). Experiments not shown are consistent with the w^{-2} dependence of τ.

At this point we will focus on the influence of channel width in the bottleneck effect and in the range of validity of the above model. Actually, by analyzing the onset of monolayer pressurization, we reveal a threshold channel width ($\simeq 400$ μm) below which the compression chamber is effectively isolated by the channel. Indeed from Eqs. (6) and (8), we derive $d\Pi/dt|_{t=0} = (\kappa L)^{-1} v_b$, independent of geometrical and viscous effects. A systematic set of experiments performed by varying w and v_b is in quantitative agreement with this result as long as $w \leq 400$ μm (see Fig. 4). Conversely, for larger widths up to the widest investigated one, $w = 3$ mm, this analysis yields an effective length of the compression compartment, $L_{\text{eff}}(w)$, steadily increasing with w. Exponentially fitted (see inset), one finds indeed that $L_{\text{eff}}(w \geq 1 \text{ cm}) \simeq 38$ cm, the total length of the cuvette. In other words, a microchannel up to 400 μm wide, under our experimental conditions, completely blocks the material continuity of the spread interface in its response to the initial drive. On the other hand, the monolayer behaves at all times as a continuous interfacial medium, extended all over the available area of the Langmuir trough, for an outlet only slightly above one tenth of the section W.

Remarkably, the relaxation of the channel velocity is seen to obey Eq. (7) for extended times after the onset. We plot in Fig. 5 the time variation of v_c for various barrier speeds v_b, and fixed w. Since there is a significant uncertainty in the effective w values for each experiment (see above), we choose to fit Eq. (7) to each data set in order to obtain characteristic relaxation rates. We find that not only can we define a characteristic time constant for each case, but also that it remains independent of v_b (see inset). Finally we emphasize that the characteristic time constant of these flow buildup experiments, the one found above in

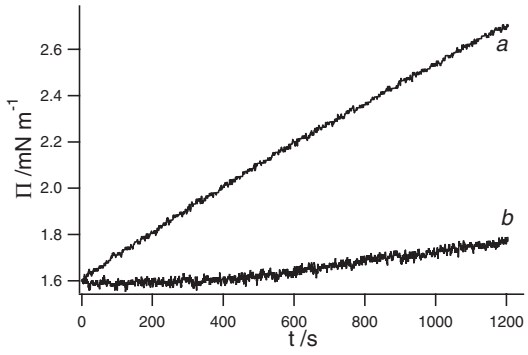

FIG. 3. Surface pressure evolution at the beginning of compression of an elaidic acid monolayer at $v_b = 0.5$ mm min^{-1} through a microchannel 0.2 mm wide in (*a*) the compression chamber and (*b*) the expansion chamber.

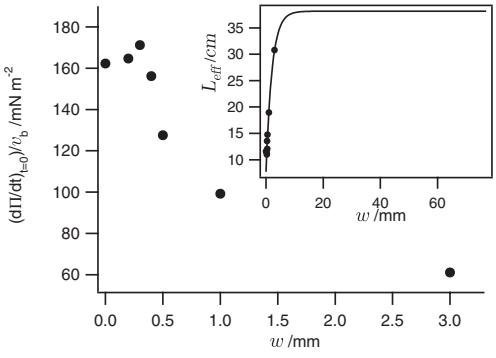

FIG. 4. Dependence of the initial surface pressure temporal slope on the compression rate when varying the channel width w. Inset shows the dependence of L_{eff} on w (see text).

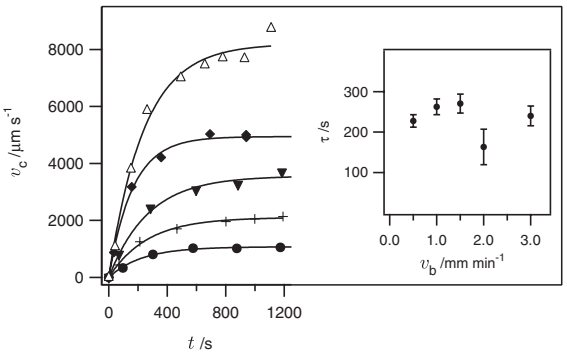

FIG. 5. Velocity transients inside a channel of nominal width 0.4 mm at different barrier velocities: 0.5, 1.0, 1.5, 2.0 and 3.0 mm min^{-1} (from bottom to top). Inset: Calculated time constant τ from a fit to Eq. (7).

the pressure relaxation experiments [Fig. 1(a)] and the value predicted by our model [Eq. (8)], are in full agreement.

In summary, we have presented the first direct analysis of the so-called bottleneck effect, ubiquitous in miniaturized flow systems. By studying the flow behavior in a Langmuir monolayer, we can directly relate the long transient behaviors to the intrinsic material compressibility, rather than to the compliance of the containing walls as it is the case in bulk microfluidics. These studies may be a starting point for the development of two-dimensional microfluidic methods, which will certainly be based on the preexisting knowledge gained from experiments of constrained flows in monolayers. Results reported here advise against the use of constant mechanical pumping, given the delayed response inside microchannels. Similarly to what is proposed in standard microfluidics, one would be thus tempted instead to propose to work under constant pressure conditions. Our experiments, however, reveal that usable velocity ranges are already originated from small gradients in surface pressure, nearing the precision of typical surface tension balances (0.1–0.2 mN m^{-1}). Consequently, an active flow velocity control taking into account the large τ values will be a better strategy than surface pressure control to generate a given velocity profile inside two-dimensional channels. Results reported here could be the basis for techniques to achieve such a goal overcoming the ubiquitous transient regimes arising from the compressibility of Langmuir monolayers. The extrapolation of such advances to two-dimensionally micromanipulated mixed monolayers, prior to their transference from aqueous to a solid support, could unveil new possibilities to assemble patterned surfaces with tailored biological or optical activity.

This work was supported by MEC through Project No. FIS2006-03525 and by DURSI through Project No. 2005SGR00653. P. B. is grateful for the support of Departament d'Educació i Universitats de la Generalitat de Catalunya and Fons Social Europeu. J. I.-M. acknowledges support from Ramón y Cajal Program (MCyT). We deeply thank Dr. P. Tabeling for fruitful discussions.

[1] G. M. Whitesides, Nature (London) **442**, 368 (2006).
[2] H. A. Stone, A. D. Stroock, and A. Ajdari, Annu. Rev. Fluid Mech. **36**, 381 (2004).
[3] P. Tabeling, *Introduction to Microfluidics* (Oxford University Press, New York, 2005).
[4] P. Tabeling, in *Proceedings of the 14th Australasian Fluid Mechanics Conference, Adelaide, Australia, 2001* (Adelaide University, Adelaide, Australia, 2001).
[5] M. Martin, G. Blu, C. Eon, and G. Guiochon, J. Chromatogr. **112**, 399 (1975).
[6] V. M. Kaganer, H. Möhwald, and P. Dutta, Rev. Mod. Phys. **71**, 779 (1999).
[7] J. Ignés-Mullol, J. Claret, R. Reigada, and F. Sagués, Phys. Rep. **448**, 163 (2007).
[8] D. A. Edwards, H. Brenner, and D. T. Wasan, *Interfacial Transport Processes and Rheology* (Butterworth-Heinemann, Boston, MA, 1991).
[9] R. Miller, R. Wüstneck, J. Krägel, and G. Kretzschmar, Colloids Surf. A **111**, 75 (1996).
[10] P. Cicuta and E. M. Terentjev, Eur. Phys. J. E **16**, 147 (2005).
[11] M. Sacchetti, H. Yu, and G. Zografi, J. Chem. Phys. **99**, 563 (1993).
[12] D. K. Schwartz, C. M. Knobler, and R. Bruinsma, Phys. Rev. Lett. **73**, 2841 (1994).
[13] H. A. Stone, Phys. Fluids **7**, 2931 (1995).
[14] M. L. Kurnaz and D. K. Schwartz, Phys. Rev. E **56**, 3378 (1997).
[15] A. Ivanova, M. L. Kurnaz, and D. K. Schwartz, Langmuir **15**, 4622 (1999).
[16] D. J. Olson and G. G. Fuller, J. Non-Newtonian Fluid Mech. **89**, 187 (2000).
[17] H. L. Welles, G. Zografi, C. M. Scrimgeour, and F. D. Gunstone, in *Monolayers*, edited by E. Goddard, Advances in Chemistry Series Vol. 144 (American Chemical Society, Washington D.C., 1975), pp. 135–153.
[18] K. Iimura, Y. Yamauchi, Y. Tsuchiya, and T. Kato, Langmuir **17**, 4602 (2001).
[19] B. M. Ocko, M. S. Kelley, A. T. Nikova, and D. K. Schwartz, Langmuir **18**, 9810 (2002).
[20] A small and constant decrease in the surface pressure is observed in both cases, probably due to a slight dissolution of the amphiphilic material.
[21] K. S. Yim, C. F. Brooks, G. G. Fuller, D. Winter, and C. D. Eisenbach, Langmuir **16**, 4325 (2000).
[22] W. S. Rasband, ImageJ, 1997–2008, http://rsb.info.nih.gov/ij/.
[23] C. Barentin, C. Ybert, J. M. di Meglio, and J.-F. Joanny, J. Fluid Mech. **397**, 331 (1999).
[24] We have used $\mu_d \simeq 10$ mN s m^{-1} [F. Monroy (private communication)] and a $\kappa \simeq 5 \times 10^{-2}$ m mN^{-1} (from our measured surface pressure versus area isotherms).